Kernel-based Time-Varying IV estimation: handle with care

Lucchetti, Riccardo and Valentini, Francesco

6 October 2021

Kernel-based Time-Varying IV estimation: handle with care

Riccardo Lucchetti
Università Politecnica
delle Marche (IT)
r.lucchetti@univpm.it

Francesco Valentini
Università Politecnica
delle Marche (IT)
f.valentini@univpm.it

Abstract

Giraitis, Kapetanios, and Marcellino (Journal of Econometrics, 2020) proposed a kernel-based time-varying coefficients IV estimator. By using entirely different code, We broadly replicate the simulation results and the empirical application on the Phillips Curve but we note that a small coding mistake might have affected some of the reported results. Further, we extend the results by using a different sample and many kernel functions; we find that the estimator is remarkably robust across a wide range of smoothing choices, but the effect of outliers may be less obvious than expected.

Keywords: Instrumental variables, Time-varying parameters, Hausman test, Phillips curve

Corresponding author: Francesco Valentini. Address: *Department of Economics and Social Sciences (DiSES), Marche Polytechnic University, Piazzale Martelli 8, 60121, Ancona (IT).*
Mail: f.valentini@univpm.it

Conflict of Interest: None

1 Introduction

The issue of estimation of linear models when the underlying data generation process may be unstable through time is a long-standing one in the econometric literature. One solution, adopted since the pioneering contribution by Chow (1960), is to assume that abrupt breaks take place at some point in time, and this idea has been extended and generalized in several directions (see *eg* Bai & Perron, 2003).

An increasingly common alternative is to assume that the model parameters change continuously through time. The standard solution is to rely on the state-space representation and use the Kalman filter apparatus under the Gaussianity assumption (see eg Hamilton, 1994, section 13.8), but other approaches have been put forward (see Schlicht, 2021, among others).

In recent years, a method has been proposed that deals with time-varying parameter models in a non-parametric way, thereby ensuring great generality and flexibility, as long as the evolution of the parameters through time can be assumed to be "slow".[1] In a series of works by Giraitis, Kapetanios and several co-authors (Giraitis, Kapetanios, & Yates, 2014; Giraitis et al., 2018; Kapetanios, Marcellino, & Venditti, 2019) the idea is pursued to generalize the concept of rolling-window regression to kernel-based inference.

One of the advantages of the Giraitis et al. (2014) approach is that it is easily generalizable to a number of linear models, among which instrumental variable models. IV models with time-varying parameters can, in principle, be handled via a state-space approach, but its implementation is far from trivial; a Bayesian alternative has been proposed by Ruisi (2019). None of these approaches, however, match the computational simplicity and flexibility of the kernel-based estimator. On the other hand, in semi- and non-parametric estimation methods one usually has to choose the precise details of the practical implementation of the estimators, and while many of these choices are equivalent asymptotically, in finite samples the numerical results are often affected to quite a large degree.

In this article, we replicate and extend the results presented in Giraitis et al. (2020) (GKM from now on), using a completely independent software implementation[2] and publicly-available data.

Our first step is to perform a narrow-sense replication of the original results: we find that the

[1] For a precise definition, see eg Giraitis, Kapetanios, and Yates (2018), sec. 2.1.

[2] The code we used for this exercise is publicly available as the `ketvals` gretl package.

simulation results can be replicated almost exactly; in fact, in some cases, our Monte Carlo results are even closer to the asymptotic figures than the original ones. The empirical application, on the New Keynesian Phillips Curve, can also be replicated satisfactorily, the main exceptions being the effects of what we believe is an unfortunate typo in the original article and slight discrepancies in the dataset.

Then, we perform an extra set of experiments on the empirical application, extending the original results in two separate directions: (a) we extend the dataset from the 1959–2013 to the full dataset 1948–2020 and examine the differences in the time paths of coefficients and other results (b) we using different kernel types and bandwidths, both for the original sample range and for the updated one. We find that results are, all in all, quite robust across different specifications; however, in some cases results can be markedly different across equally legitimate choices. Moreover, we find that replicating the empirical exercise with more recent data, that includes the recent COVID pandemic, sheds some light on the behavior of the estimator when large outliers are present. Therefore, it is advisable for practitioners to take great care with the robustness of their results.

2 The model

We consider the model, for $t = 1 \dots T$,

$$\begin{cases} y_t = \boldsymbol{x}_t' \boldsymbol{\beta}_t + u_t \\ \boldsymbol{x}_t = \boldsymbol{z}_t' \boldsymbol{\psi}_t + \boldsymbol{\nu}_t \end{cases} \tag{1}$$

where y_t is the dependent variable, $\boldsymbol{x}_t$ is a $p \times 1$ vector of (possibly endogenous) regressors, $\boldsymbol{z}_t$ denotes a $q \times 1$ vector of instruments and the parameters $\boldsymbol{\beta_t}$ and $\boldsymbol{\psi}_t$ are allowed to vary over time. The coefficients are assumed to be either smoothly varying deterministic functions (see Assumption 2 in GKM) or smoothly varying persistent stochastic processes (see Assumption 3 in GKM).

We denote $0 \leq r \leq p$ the number of elements of $\boldsymbol{x}_t$ that are deemed to be endogenous, so $\boldsymbol{x}_t$ and $\boldsymbol{z}_t$ have $(p-r)$ elements in common. Finally, u_t and $\boldsymbol{\nu}_t$ are the disturbances: of course, endogeneity can be described as non-zero correlation between u_t and $\boldsymbol{\nu}_t$.

In this paper we focus on two different estimators proposed in GKM:

1. The time-varying OLS estimator

$$\hat{\boldsymbol{\beta}}_t = \left(\sum_{j=1}^{T} b_{H,|j-t|} \boldsymbol{x}_j \boldsymbol{x}_j' \right)^{-1} \left(\sum_{j=1}^{T} b_{H,|j-t|} \boldsymbol{x}_j y_j \right) \tag{2}$$

2. The time-varying IV estimator[3]

$$\tilde{\boldsymbol{\beta}}_t = \left(\sum_{j=1}^{T} b_{H,|j-t|} \hat{\boldsymbol{\psi}}_j' \boldsymbol{z}_j \boldsymbol{x}_j' \right)^{-1} \left(\sum_{j=1}^{T} b_{H,|j-t|} \hat{\boldsymbol{\psi}}_j' \boldsymbol{z}_j y_j \right) \tag{3}$$

where $b_{H,|j-t|} = K\left(\frac{|j-t|}{H}\right)$ is a kernel weight with bandwidth parameter $H = T^{h_1}$ and $\hat{\boldsymbol{\psi}}_t$ is used to indicate the time-varying first-stage OLS estimates of $\boldsymbol{\psi}_t$, possibly allowing for a different kernel bandwidth $L = T^{h_2}$ in the first stage regression. In the original article, another IV estimator is also analyzed, namely $\tilde{\boldsymbol{\beta}}_{2,t} = \left(\sum_{j=1}^{T} b_{H,|j-t|} \hat{\boldsymbol{\psi}}_t' \boldsymbol{z}_j \boldsymbol{x}_j'\right)^{-1} \left(\sum_{j=1}^{T} b_{H,|j-t|} \hat{\boldsymbol{\psi}}_t' \boldsymbol{z}_j y_j\right)$, that is asymptotically equivalent to $\tilde{\boldsymbol{\beta}}_t$; however, we do not consider it in our replication since the empirical application focuses on $\tilde{\boldsymbol{\beta}}_t$, which appears to be the preferred form.

GKM also define a time-varying equivalent of the classic Hausman test, whose statistic is given by the following quadratic form:

$$\frac{K_t^2}{K_{2,t}} V_{T,t}' \hat{\Sigma}_{\hat{\nu}\hat{\nu},t}^{-1} V_{T,t} \hat{\sigma}_{\hat{u},t}^{-2} \xrightarrow{\text{p}} \chi_r^2, \tag{4}$$

where

$$\begin{aligned}
&K_t = \textstyle\sum_{j=1}^{T} b_{H,|j-t|}; && K_{2,t} = \textstyle\sum_{j=1}^{T} b_{H,|j-t|}^2; \\
&\hat{\Sigma}_{\hat{\nu}\hat{\nu},t} = K_t^{-1} \textstyle\sum_{j=1}^{T} b_{H,|j-t|} \hat{\nu}_j \hat{\nu}_j'; && \hat{\sigma}_{\hat{u},t}^2 = K_t^{-1} \textstyle\sum_{j=1}^{T} b_{H,|j-t|} \hat{u}_j; \\
&V_{T,t} = \left(\textstyle\sum_{j=1}^{T} b_{H,|j-t|} \hat{\boldsymbol{x}}_j \hat{\boldsymbol{x}}_j'\right)^{1/2} \left(\textstyle\sum_{j=1}^{T} b_{H,|j-t|} \boldsymbol{x}_j \boldsymbol{x}_j'\right)^{1/2} \left(\tilde{\boldsymbol{\beta}}_t - \hat{\boldsymbol{\beta}}_t\right) \quad .
\end{aligned}$$

and $\hat{\nu}_j$ and $\hat{u}_j$ denote the of the first- and second-stage residuals, respectively, and $\hat{\boldsymbol{x}}_j$ are the first-stage fitted values.

Note that, according to the notation in GKM, the degrees of freedom of the χ^2 limiting distribution of the Hausman test statistic is given as p, the number of explanatory variables (equation (35) in GKM), while in fact it should be equal to the number of potentially endogenous variables

[3]Denoted $\tilde{\beta}_{1,t}$ in the original work.

r (see e.g., Davidson & MacKinnon, 1999, Section 8.7). Unfortunately, it looks as if this trivial typo made its way into the code used by the authors and affected some of their results; we will investigate this issue in Section 3.2.

In the same vein, GKM also propose a "Global Hausman Test" for a given time span $[T_0, T_1]$, defined as

$$\mathcal{H}_{T_0,T_1} = \frac{1}{\sqrt{T_1 - T_0}} \sum_{t=T_0+1}^{T_1} K_t K_{2,t}^{-1} \hat{\sigma}^{-1} \hat{\Sigma}_{\hat{\nu}\hat{\nu},t}^{-1/2} V_{T,t},$$

$$H = \mathcal{H}'_{T_0,T_1} \mathcal{H}_{T_0,T1} \xrightarrow{\text{p}} \chi^2_r \tag{5}$$

where a similar remark on the degrees of freedom of the test applies.

3 Narrow-sense Replication

In this section we report the results concerning the narrow-sense replication of the results in GKM. We first show the Monte Carlo experiment and then we focus on the empirical application.

3.1 Simulations

In the first part of their article, GKM perform a series of simulation experiments on the univariate DGP $y_t = \beta x_t + u_t$ to assess the quality of the time-varying OLS and IV estimators over a range of possible data generating processes. We report the simulation design in Appendix A. Suffice it to say here that 96 basic scenarios are considered, stemming from the possible combinations of (a) exact identification vs over-identification (b) degree of endogeneity of the x_t explanatory variable: none, moderate and strong (c) sample size $T = 100, 200, 400, 1000$ (d) bandwidth choice: $h_1 = 0.4, 0.5$ and $h_2 = 0.4, 0.5$. As in the original article, the number of Monte Carlo replications is set to 1000.

The indicators used to assess the performance of the estimators are: (1) item median deviation; (2) item absolute median deviation; (3) item interdecile range, and (4) item 95% coverage rate. The full set of results is reported in Appendix A; here, we just briefly remark that indicators 1 and 2 are broadly consistent with those of GKM, apart from the OLS endogeneity bias being slightly larger in the just-identified case. On the contrary, the decile range is narrower in our simulation for

both OLS and IV, which seems to indicate higher efficiency than reported in the original article.[4] As for indicator 4 (the 95% coverage rate), the figures we find are closer to the nominal value for the IV estimator.

For the Global Hausman Test, we have a slightly larger rejection rate (closer to the nominal level) under the null compared to the original results, but apart from this we are able to replicate Table 8 in GKM almost perfectly. It is worth noting, however, that in this case $p = r$ by design, so the typo in Equation (4) is inconsequential.

3.2 Empirical Application: the Phillips Curve

In this section, we replicate the empirical application reported in section 4 of GKM, where a time-varying version of the Phillips curve is estimated. The following two models are considered: a "traditional", backward-looking version

$$\Delta\pi_t = \mu_t + \gamma_t \Delta\pi_{t-1} + \alpha_t \Delta u_t, \tag{6}$$

and a "New-Keynesian" forward-looking version

$$\Delta\pi_t = \mu_t + \gamma_t \Delta\pi_{t-1} + \alpha_t \Delta u_t + \rho_t \Delta\pi_{t+1}. \tag{7}$$

Here, $\Delta\pi_t$ and Δu_t are the first differences of inflation and unemployment, respectively. The aim of the analysis is to ascertain whether unemployment is significant and endogenous and how these characteristics evolve over time. The original article does not point to a downloadable dataset, but we consider the usage of the St. Louis FED data as a reasonable reconstruction. To be specific, we compute inflation π_t as 100 times the seasonal log difference of the `CPIAUCSL` variable; unemployment u_t is simply a copy of the `UNRATE` variable. As for the exact sample range, we use the sample from 1959:02 to 2013:07.

In the first example, Δu_t is considered endogenous and the additional instruments are the lags of Δu_t from order 1 to 4. In the second model, $\Delta\pi_{t+1}$ is also considered endogenous and the set of instruments includes four lags of Δu_t and four lags of $\Delta\pi_t$. Figure 1 shows the replication

[4] We believe there is a little editorial issue in the original article: in Tables 1–6, rows 4–8 seem to be swapped with rows 9–12.

results, where the "traditional" and the "New-Keynesian" Phillips curves are reported by columns. The estimated coefficients for $\hat{\boldsymbol{\beta}}_t$ and $\tilde{\boldsymbol{\beta}}_t$, with their 90% confidence intervals[5] and the Hausman test p-value are reported by row. Both models are estimated using $h_1 = h_2 = 0.7$ as bandwidth parameters.

[FIGURE 1 ABOUT HERE]

For Equation (6), the time paths of estimated coefficients and the associated confidence bands can be replicated almost exactly. We note only very minor discrepancies near the end of the sample, which can safely attributed to differences in the data vintage used. On the other hand, the plot for the time-varying Hausman test appears to be rather different, with much lower p-values for the best part of the sample. We believe this discrepancy might be due to the incorrect number of degrees of freedom of the limiting χ^2 distribution in GKM. To substantiate our claim, Figure 2 compares the time path of the p-value for the Hausman test obtained using the correct number of degrees of freedom ($r = 1$) and the one obtained using the total number of regressors ($p = 3$). As can be seen, the time path of the p-value with 3 degrees of freedom is much closer to the one reported in GKM at the end of Section 4.

[FIGURE 2 ABOUT HERE]

As for the "New-Keynesian" Phillips curve in Equation (7), we observe noticeable differences between our results and the original GKM ones. For the three parameters in the model, we are able to almost perfectly replicate the time path and the confidence intervals of the least squares estimator $\hat{\boldsymbol{\beta}}_t$. On the contrary, the IV estimates appear to be quite different all over the sample, particularly at the beginning and the end of the sample. Since the differences in the OLS estimates are relatively minor and can safely be attributed to the different data vintage we use, we conjecture that the IV estimator, in an over-identified case such as the present one, may be somewhat sensitive to individual data points. This conjecture is consistent with the evidence we present in Section 4.2, where we show the effects on the estimator of one extreme outlier, given by the unemployment

[5] In order to picture both estimators in the same plot, we follow the same graphical style as GKM: the OLS estimates are in red and the IV ones are in blue. Straight lines represent the coefficients, dotted lines denote confidence intervals.

surge of April 2020. Given these premises, it is obvious that the Hausman test results could not be replicated satisfactorily.

Finally, in order to provide the complete set of the results shown by GKM, Figure 8 in Appendix B reports the replication of the robustness check exercise on the "traditional" Phillips curve, where the parameters h_1 and h_2 are set to 0.5. Similarly to our previous results, the time paths of the estimated coefficients are very similar to the reported ones, although the Hausman p-value plot is not.

4 Extended replication

In this section, we extend the empirical example of the original article by investigating robustness of results with respect to two separate issues, namely (a) different choices of the kernel weighting scheme and (b) an extension of the sample used by the authors. As will be argued, both these aspects reveal interesting features of the estimator.

4.1 Kernel functions and bandwidth

In this subsection, we investigate the sensitivity of the results to the choice of the kernel function and the bandwidth parameters: we replicate the empirical analysis provided in Section 3.2 by using four different kernel functions, namely the Gaussian, Epanechnikov and exponential kernels, as well as the rectangular kernel, which is equivalent to a simple rolling-window estimator.

The Gaussian kernel is the one used by GKM in the original paper, and the kernel weigthing function is proportional to a Gaussian density $K(x) = \exp(-x^2/2)$, where $x = |j - t|/T^h$. The exponential kernel is very similar, in that it uses the Laplace density instead: $K(x) = \exp(-|x|)$.[6] These two kernel choices have infinite support, so that all observations in the sample contribute to the calculation of each element of the $\hat{\boldsymbol{\beta}}_t$ and $\tilde{\boldsymbol{\beta}}_t$ sequences. The other two kernels, instead, have finite support: for $|x| < 1$, $K(x) = 0.75(1 - x^2)$ for the Epanechnikov kernel and $K(x) = 1$ for the rectangular one; both are 0 for $|x| \geq 1$. This implies that in the calculation of $\hat{\boldsymbol{\beta}}_t$ and $\tilde{\boldsymbol{\beta}}_t$ only "nearby" data matter. As will be seen, the distinction between the two kinds has noticeable empirical implications.

[6] In fact, more general formulations are possible: GKM, in the original paper, consider using $K(x) = \exp(-c \cdot |x|^\alpha)$.

Figure 3 reports the estimated coefficients, together with their confidence intervals, and the Hausman test p-value for the model in Equations (6). As a benchmark, we consider the same bandwidth parameters used in the original paper, that is $h_1 = h_2 = 0.7$.

[FIGURE 3 ABOUT HERE]

At first glance, the results appear to be qualitatively robust to the choice of kernels. Magnitude of coefficients and confidence intervals are similar across the different smoothing functions, even though estimates relying on finite support kernels (i.e., rolling window and Epanechnikov) exhibit a higher time-variability, spiky confidence intervals and provide a more unstable results over time for the Hausman test, compared to the coefficients obtained with infinite support kernel functions.

[FIGURE 4 ABOUT HERE]

Figure 4 reports the same set of estimates shown in Figure 3 obtained by setting the bandwidth parameters to $h_1 = h_2 = 0.5$. Here too, the time path of all the estimators appears to be quite unstable, even though point estimates are comparable to those in Figure 4. On the contrary, confidence intervals and the Hausman test are rather sensitive to the bandwidth choice: estimates obtained by using finite-support kernels appear to be volatile at the end of the sample and the time-varying p-value for the Hausman test is markedly unstable.

4.2 Extending the sample

We now investigate the effects of a sample extension. Figure 5 shows the results for model in Equation (6) based on observations ranging from 1948:06 to 2021:03 from the St. Louis FED dataset. This experiment is particularly interesting, because it includes data from the COVID-19 pandemic. As we will show, this provides a very interesting "natural experiment" to evaluate the performance of the estimator under extreme conditions.[7]

The results we obtain from this experiment, in terms of the robustness of results, are mixed. On the one hand, the parameter estimates appear to be strongly robust to the choice of the time span, apart form small and obvious differences around 1960 and 2013 due to the fact that we add

[7]Clearly, the 2020 unemployment spike had nothing to do with changing structural coefficients and everything to do with an exogenous shock that had a dramatic impact on unemployment but a negligible impact on inflation. However, we believe this is a perfect illustration of the numerical consequences on the estimates of one large outlier.

new observations at the beginning and at the end of the sample. On the other hand, estimated standard errors seem to be quite different from the original ones even within the period considered by GKM. Using infinite support kernels (that is, Gaussian and exponential kernels) the confidence intervals for the parameter α_t in the late 1990s appear much larger than the original ones.

[FIGURE 5 ABOUT HERE]

This is hardly surprising, given that the standard errors for the IV parameters depend on the first stage residuals: extending the sample so as to include the COVID pandemic period has a dramatic effect on the estimated standard errors. In order to show this effect, Figure 6 reports IV estimates for α_t and first stage residuals for Δu_t obtained by excluding the COVID-19 period (left) and by using the full sample to 2021:3 (right). Both estimates were obtained by using the original choices by GKM, that is, Gaussian kernel and $h = 0.7$.

In the pre-COVID sample, residuals do not contain any outliers and the confidence interval of the coefficient is very similar to the one in GKM. When using the full dataset, instead, the first-stage residuals display a huge spike in April 2020, as an effect of the unemployment surge during the first wave of the pandemic: clearly, this produces an effect on standard errors for all the nearby observations which did not appear if we exclude the COVID-19 period. With an infinite-support kernel, this extends far beyond what could be considered intuitive. Note that the standard error for α_t reaches its maximum around the year 2000, ie nearly 20 years *before* the pandemic.

[FIGURE 6 ABOUT HERE]

On the other hand, the Hausman test performs satisfactorily in terms of robustness and provides the same results whatever the sample, with substantial discrepancies in the results obtained only with a Rolling Window kernel during 60's and 80's.

Note that the adverse effects shown above are somewhat mitigated by kernel choices that put a greater weight on "local" data when calculating the time-varying quantities: for example, a Gaussian kernel with a narrower bandwidth (see Figure 7). Our overall impression is that, in normal times, the estimator is quite robust across a wide range of possible choices, but in the presence of possible abrupt breaks or otherwise exceptional events much care is needed by the investigator when choosing the precise details of the smoothing kernel to use.

[FIGURE 7 ABOUT HERE]

5 Conclusions

We have presented a replication of the results provided by Giraitis et al. (2020) for their kernel-based instrumental variable regression estimator, both in a narrow and a wide sense.

In the narrow sense replication, the Monte Carlo experiment and the real data application on the Phillips Curve are replicated almost exactly. As for the empirical example, we came across a possible coding mistake which might have affected the Hausman test results proposed in the original article.

The wide sense replication focuses on the robustness of the results to different aspects: we employ different kernel functions, as well as a larger sample and show the effects on the results. We find that parameter estimates are, in general, strongly robust. On the contrary, the standard errors and the Hausman test appear to be quite sensitive to the bandwidth parameter and to the presence of extreme shocks in the series considered, such as the COVID-19 pandemic period.

In conclusion, we believe that the time-varying IV estimator put forward by GKM is a very valuable tool that displays remarkable robustness properties under general conditions. However, it is advisable to carry out a comprehensive set of robustness checks in empirical applications, since the consequences of data outliers and/or kernel weighting choices may be far from obvious.

References

Bai, J., & Perron, P. (2003). Critical values for multiple structural change tests. *The Econometrics Journal*, *6*(1), 72–78.

Chow, G. C. (1960). Tests of equality between sets of coefficients in two linear regressions. *Econometrica*, *28*, 591–605.

Davidson, R., & MacKinnon, J. G. (1999). *Econometric theory and methods*. Oxford University Press.

Giraitis, L., Kapetanios, G., & Marcellino, M. (2020). Time-varying instrumental variable estimation. *Journal of Econometrics*, *forthcoming*. doi:10.1016/j.jeconom.2020.08.013

Giraitis, L., Kapetanios, G., & Yates, T. (2014). Inference on stochastic time-varying coefficient models. *Journal of Econometrics*, *179*(1), 46-65. doi:10.1016/j.jeconom.2013.10.009

Giraitis, L., Kapetanios, G., & Yates, T. (2018). Inference on multivariate heteroscedastic time varying random coefficient models. *Journal of Time Series Analysis*, *39*(2), 129–149. doi:10.1111/jtsa.12271

Hamilton, J. (1994). *Time series econometrics.* Princeton University Press Princeton, NJ.

Kapetanios, G., Marcellino, M., & Venditti, F. (2019). Large time-varying parameter vars: A nonparametric approach. *Journal of Applied Econometrics*, *34*(7), 1027–1049.

Ruisi, G. (2019). *Time-varying local projections* (Working Papers No. 891). Queen Mary University of London, School of Economics and Finance.

Schlicht, E. (2021). Vc: a method for estimating time-varying coefficients in linear models. *Journal of the Korean Statistical Society*, 1–33.

Figure 1: Replication, $h_1 = h_2 = 0.7$

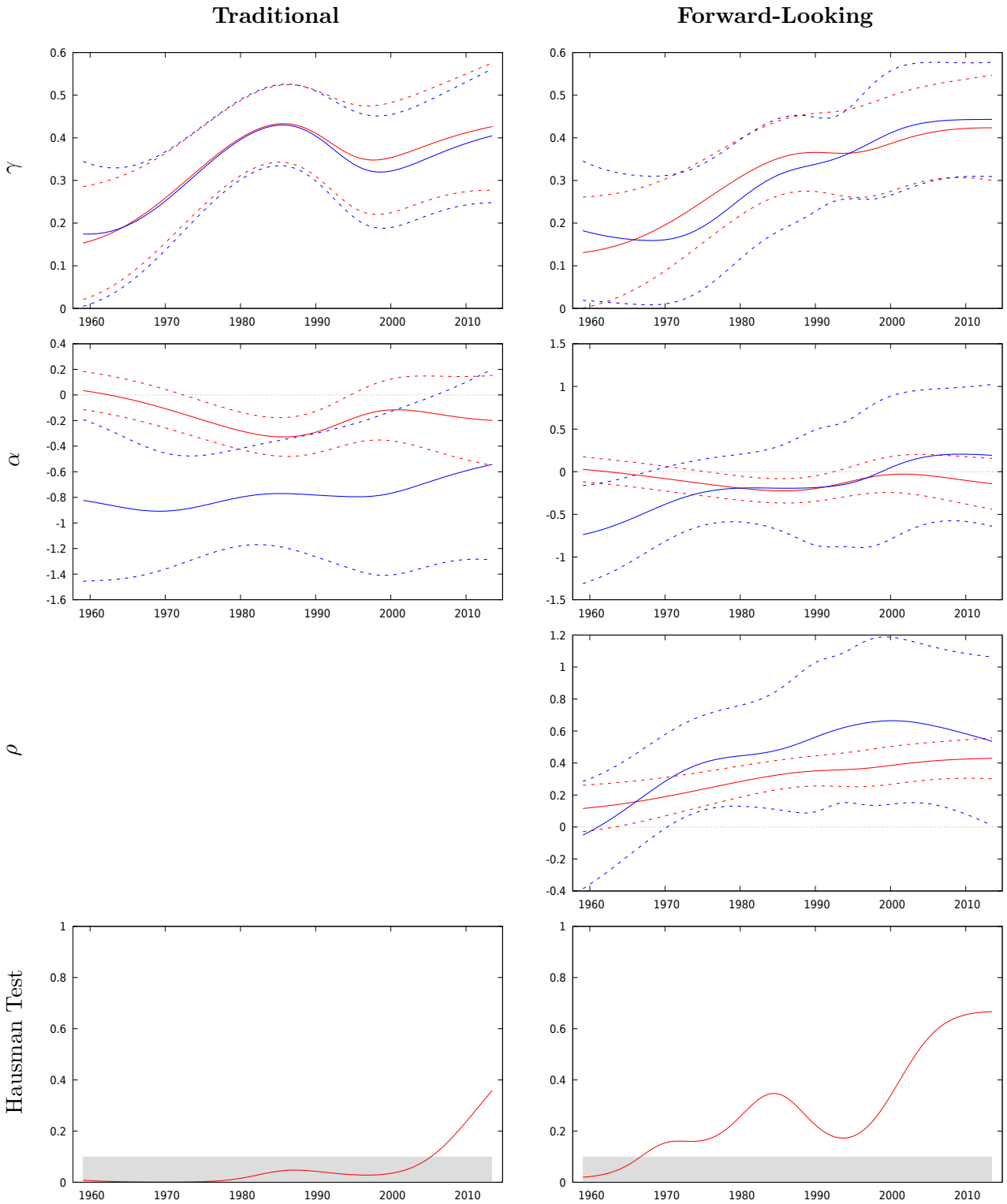

Note: the two columns report estimated coefficients and the Hausman test (p-value) related to Equations (6) and (7), respectively. With reference to coefficients, the red line denotes the OLS point estimates while the blue one represents the IV estimator. Dotted lines, with the same colors, represent the boundaries of the 90% confidence intervals. Shaded area denotes the region for p-value $\leq 10\%$.

Figure 2: Hausman test: comparing degrees of freedom

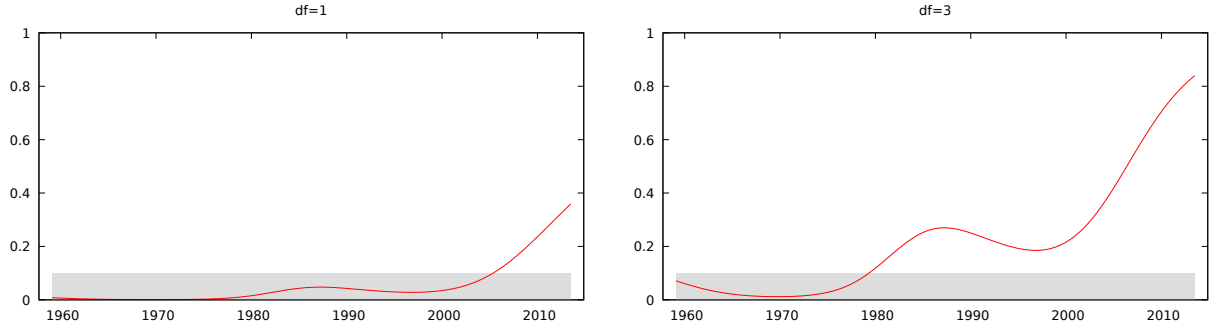

Note: the two panels report the Hausman test p-value related to the model in Equation (6), assuming a limiting χ^2-distribution with 1 (left) and 3 (right) degrees of freedom. Shaded area denotes the region for p-value $\leq 10\%$.

Figure 3: Traditional PC: 1959:02 - 2013:07, $h_1 = h_2 = 0.7$

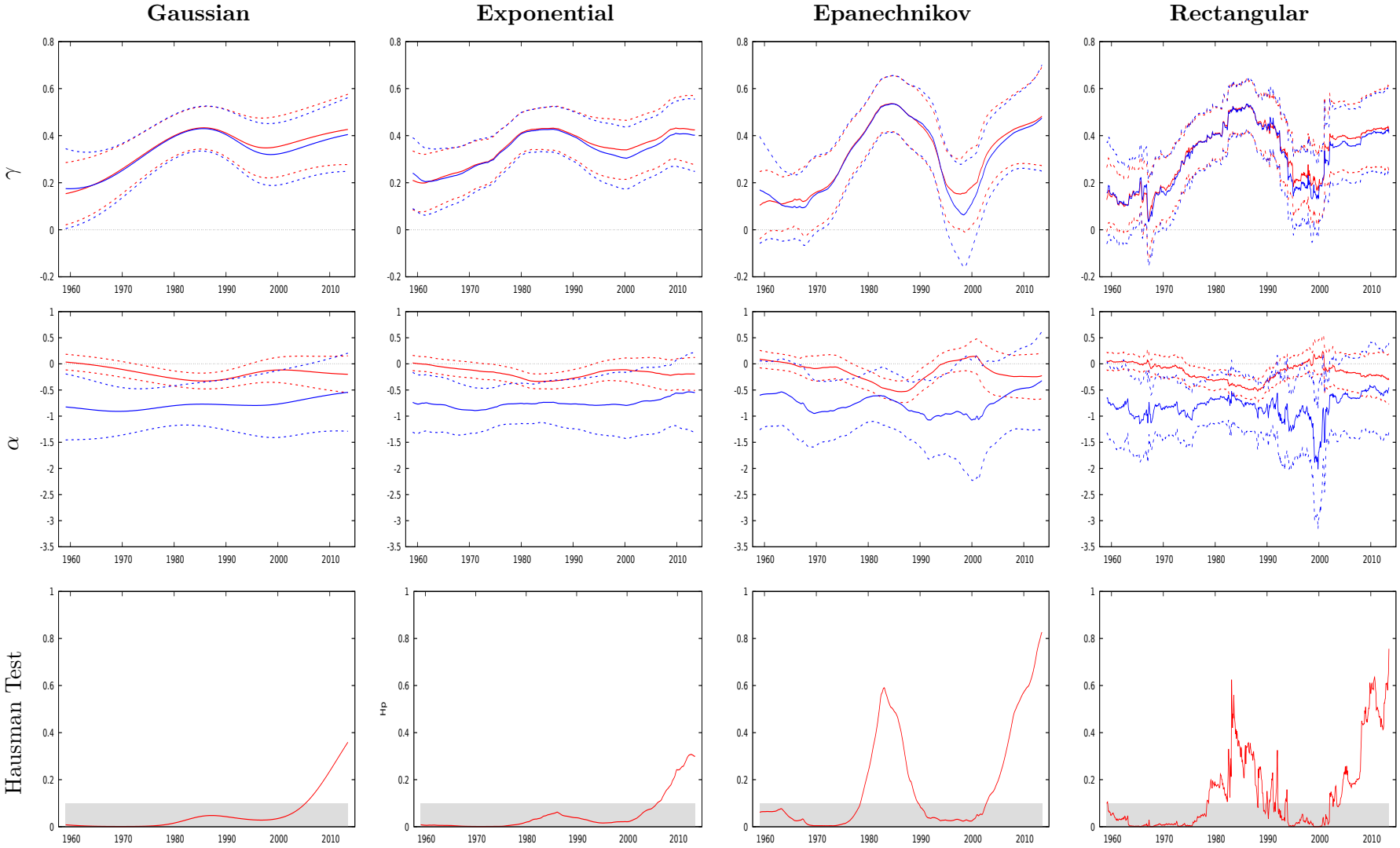

Note: Each column reports estimated coefficients and the Hausman test (p-value) related to Equation (6). With reference to coefficients, the red line denotes the OLS point estimates while the blue one represents the IV estimator. Dotted lines, with the same colors, represent the boundaries of the 90% confidence intervals.

Figure 4: Traditional PC: 1959:02 - 2013:07, $h_1 = h_2 = 0.5$

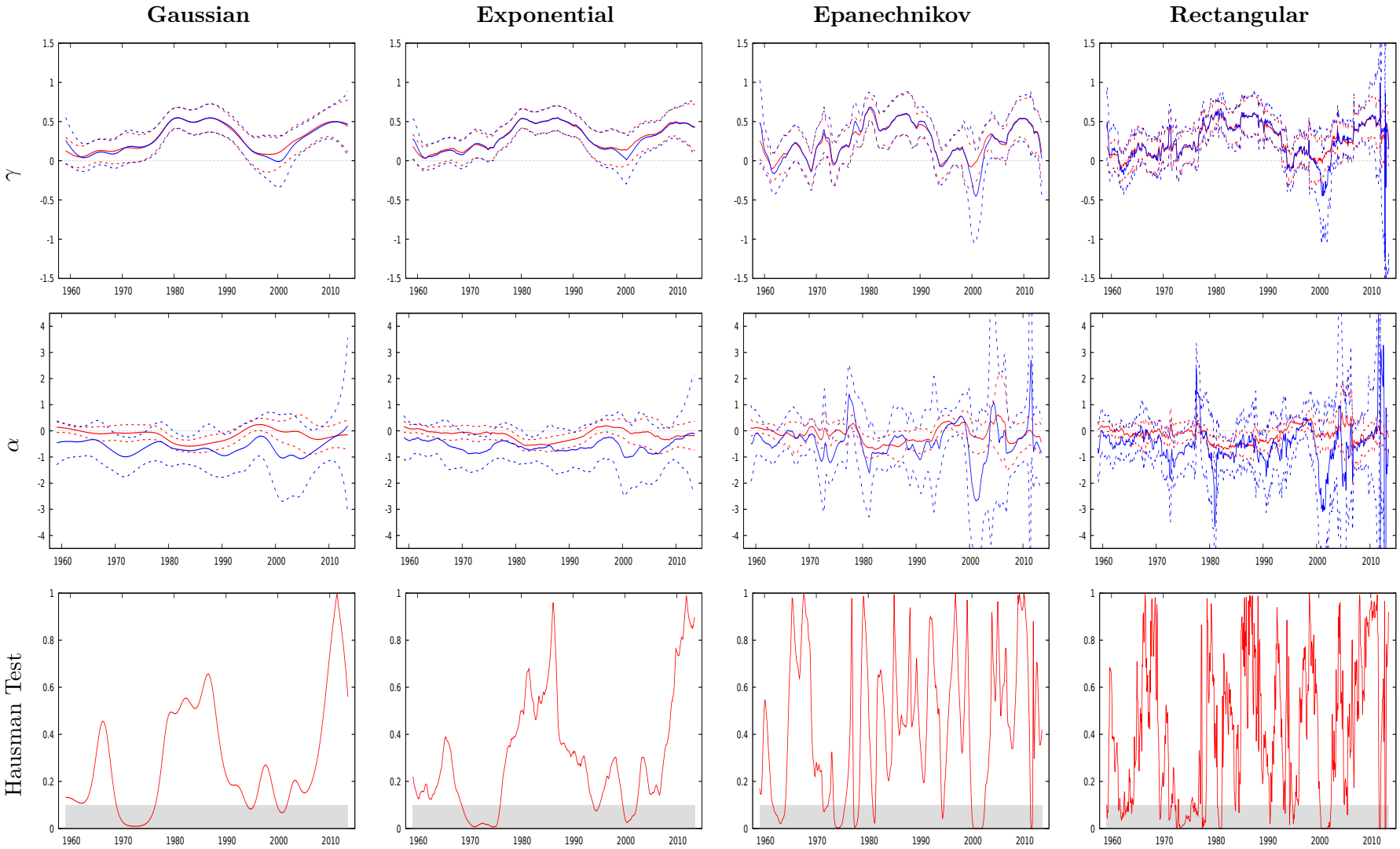

Note: see Figure 3

Figure 5: Traditional PC: 1948:06 - 2021:03, $h_1 = h_2 = 0.7$

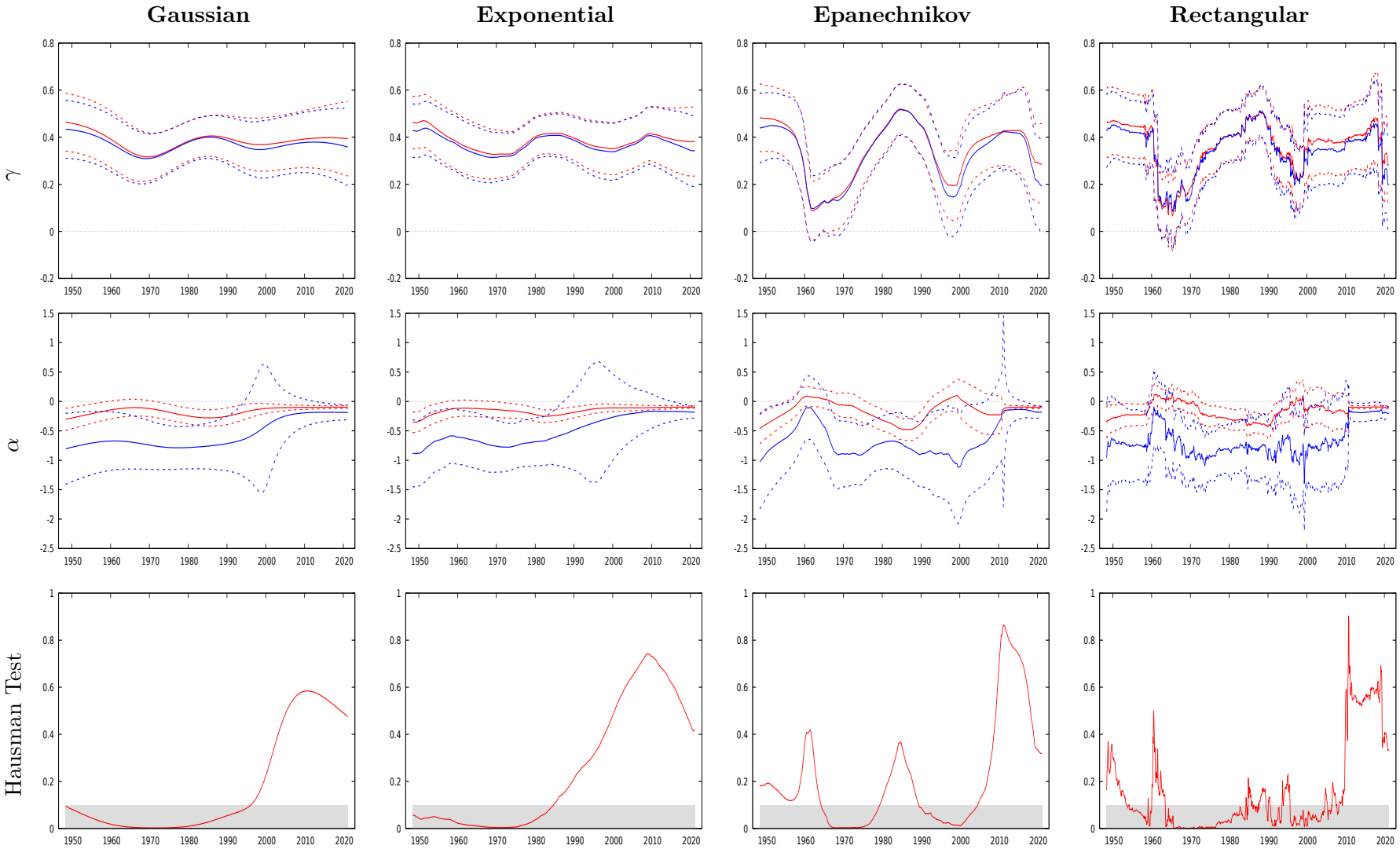

Note: see Figure 3

Figure 6: Excluding Covid-19

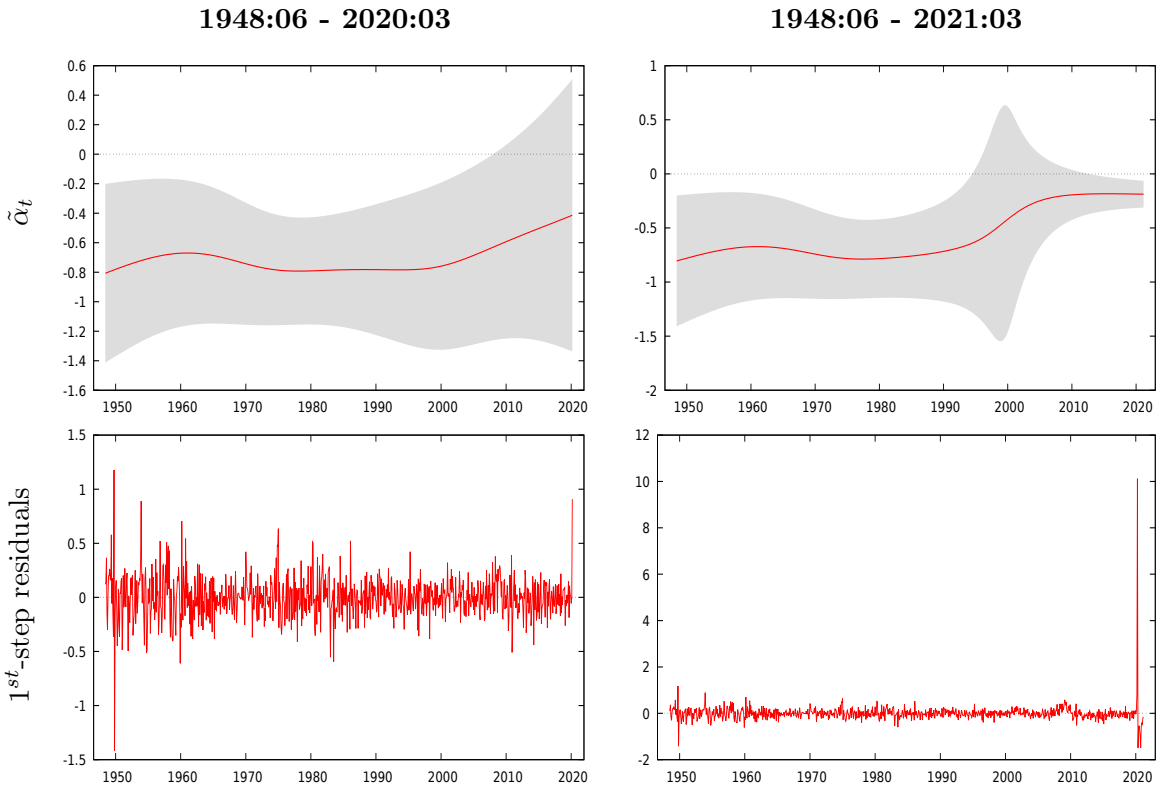

Note: the two columns report IV estimates and first-stage residuals of the endogenous variable Δu_t, obtained by excluding (left) the Covid-19 period and with the full sample (right). Gaussian kernel function, bandwidth parameters $h_1 = h_2 = 0.7$. Shaded area denotes 90% confidence interval.

Figure 7: Bandwidth: local effects on standard errors

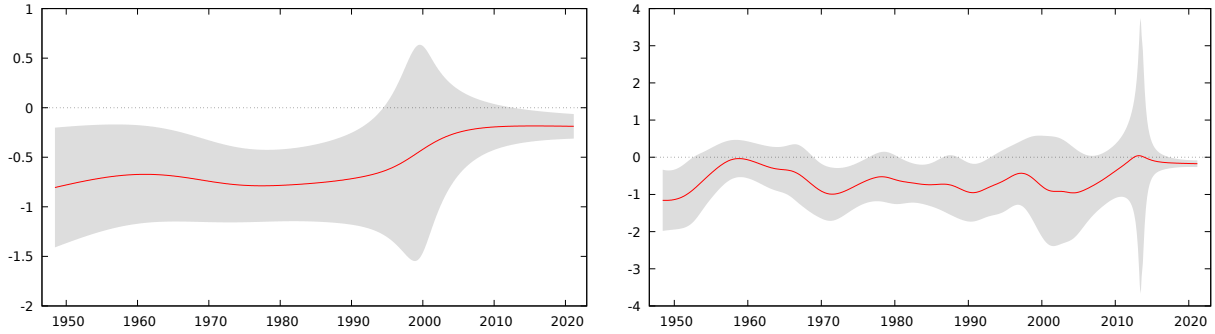

Note: the two panels report estimated $\tilde{\alpha}_t$ and 90% confidence intervals for the model in Equation (6), the kernel is Gaussian. The left panel is obtained with $h_1 = h_2 = 0.7$ and right one with $h_1 = h_2 = 0.5$. Shaded area denotes 90% confidence interval.

Appendices

A Simulation results

GKM propose two simulation designs based on the model in Equation (1). The first is one is a just-identified model of the type

$$y_t = x_t\beta_t + u_t, \quad x_t = z_t\psi_t + \nu_t, \quad t = 1, \ldots, T\,, \tag{8}$$

while the second one is an over-identified model

$$y_t = x_t\beta_t + u_t, \quad x_t = z_{1,t}\psi_{1,t} + z_{2,t}\psi_{2,t} + \nu_t, \quad t = 1, \ldots, T. \tag{9}$$

where y_t is the dependent variable, x_t is an explanatory variable and $z_{\cdot,t}$ is the instrument; all are drawn from a Gaussian distribution. The error terms, u_t and ν_t are generated according to

$$u_t = se_{1,t} + (1-s)e_{2,t}, \quad \nu_t = se_{1,t} + (1-s)e_{3,t}\,,$$

where $s = \{0, 0.2, 0.5\}$ governs the correlation between the error terms and where $e_{\cdot,t}$ denotes an i.i.d. Gaussian sequence. Finally, the parameters β_t, $\psi_{1,t}$ and $\psi_{2,t}$ follow a $\sqrt{T}$-rescaled random-walks.

In the following tables, we report for $\hat{\beta}_t$ and $\tilde{\beta}_{1,t}$ the Monte Carlo average of the Median Deviation, the Absolute Median Deviation, the Decile Range and the Coverage range of the 95% C.I. based on estimated standard errors. Each table is referred to a different design and includes different scenarios concerning the sample size T and the bandwidth parameters h_i and h_2.

See Giraitis et al. (2020) for further details.

Table 1: Just-Identified Case, $s = 0$

h_1	h_2	T	Median Deviation		Abs. Med. Dev.		Decile Range		95% Coverage	
			$\hat{\beta}_t$	$\tilde{\beta}_{1,t}$	$\hat{\beta}_t$	$\tilde{\beta}_{1,t}$	$\hat{\beta}_t$	$\tilde{\beta}_{1,t}$	$\hat{\beta}_t$	$\tilde{\beta}_{1,t}$
0.4	0.4	100	0.001	-0.005	0.162	0.338	1.018	1.698	0.826	0.938
	0.4	200	-0.001	-0.005	0.134	0.292	1.034	1.596	0.848	0.944
	0.4	400	0.002	0.001	0.114	0.255	1.021	1.520	0.863	0.949
	0.4	1000	-0.000	-0.002	0.091	0.219	1.018	1.451	0.882	0.954
0.4	0.5	100	-0.006	-0.014	0.163	0.403	1.034	2.377	0.825	0.940
	0.5	200	-0.002	0.001	0.136	0.343	1.032	2.114	0.847	0.944
	0.5	400	-0.001	-0.009	0.112	0.298	1.039	1.976	0.868	0.949
	0.5	1000	-0.001	-0.003	0.090	0.247	1.020	1.785	0.887	0.949
0.5	0.4	100	-0.003	-0.007	0.157	0.289	0.879	1.208	0.775	0.912
	0.4	200	-0.003	-0.007	0.129	0.240	0.921	1.220	0.790	0.922
	0.4	400	-0.000	-0.000	0.106	0.201	1.002	1.243	0.797	0.920
	0.4	1000	0.000	0.003	0.083	0.168	0.949	1.152	0.803	0.918
0.5	0.5	100	-0.003	-0.006	0.158	0.321	0.877	1.415	0.778	0.924
	0.5	200	0.002	0.003	0.130	0.267	0.930	1.375	0.787	0.925
	0.5	400	0.001	-0.002	0.107	0.224	0.974	1.337	0.793	0.922
	0.5	1000	-0.000	-0.001	0.082	0.186	0.958	1.285	0.808	0.928

Table 2: Just-Identified Case, $s = 0.2$

h_1	h_2	T	Median Deviation		Abs. Med. Dev.		Decile Range		95% Coverage	
			$\hat{\beta}_t$	$\tilde{\beta}_{1,t}$	$\hat{\beta}_t$	$\tilde{\beta}_{1,t}$	$\hat{\beta}_t$	$\tilde{\beta}_{1,t}$	$\hat{\beta}_t$	$\tilde{\beta}_{1,t}$
0.4	0.4	100	0.042	0.021	0.161	0.297	1.019	1.564	0.805	0.921
	0.4	200	0.043	0.011	0.134	0.259	1.027	1.503	0.833	0.930
	0.4	400	0.041	0.004	0.114	0.228	1.019	1.421	0.848	0.939
	0.4	1000	0.042	0.006	0.094	0.197	1.032	1.380	0.862	0.945
0.4	0.5	100	0.041	-0.009	0.162	0.349	1.028	2.089	0.808	0.920
	0.5	200	0.043	-0.000	0.135	0.296	1.025	1.929	0.829	0.930
	0.5	400	0.040	0.002	0.112	0.260	1.010	1.784	0.851	0.936
	0.5	1000	0.042	0.005	0.092	0.215	1.017	1.614	0.862	0.938
0.5	0.4	100	0.043	0.005	0.160	0.258	0.879	1.109	0.752	0.893
	0.4	200	0.041	0.015	0.130	0.216	0.924	1.155	0.767	0.903
	0.4	400	0.042	0.010	0.110	0.184	0.949	1.141	0.763	0.896
	0.4	1000	0.041	0.013	0.087	0.149	0.981	1.127	0.762	0.899
0.5	0.5	100	0.039	0.007	0.157	0.289	0.877	1.342	0.760	0.910
	0.5	200	0.043	0.002	0.129	0.237	0.923	1.282	0.772	0.909
	0.5	400	0.042	0.005	0.109	0.201	0.967	1.286	0.760	0.901
	0.5	1000	0.042	0.004	0.087	0.165	0.959	1.209	0.764	0.908

Table 3: Just-Identified Case, $s = 0.5$

h_1	h_2	T	Median Deviation		Abs. Med. Dev.		Decile Range		95% Coverage	
			$\hat{\beta}_t$	$\tilde{\beta}_{1,t}$	$\hat{\beta}_t$	$\tilde{\beta}_{1,t}$	$\hat{\beta}_t$	$\tilde{\beta}_{1,t}$	$\hat{\beta}_t$	$\tilde{\beta}_{1,t}$
0.4	0.4	100	0.332	0.081	0.337	0.282	1.017	1.414	0.419	0.896
	0.4	200	0.330	0.070	0.332	0.243	1.039	1.413	0.346	0.904
	0.4	400	0.330	0.051	0.330	0.211	1.022	1.357	0.271	0.913
	0.4	1000	0.326	0.042	0.327	0.173	1.074	1.323	0.178	0.921
0.4	0.5	100	0.335	0.056	0.341	0.330	0.987	1.976	0.416	0.901
	0.5	200	0.327	0.046	0.329	0.270	1.028	1.761	0.349	0.906
	0.5	400	0.330	0.032	0.330	0.231	1.042	1.646	0.267	0.916
	0.5	1000	0.330	0.023	0.330	0.189	1.052	1.508	0.176	0.923
0.5	0.4	100	0.321	0.078	0.329	0.248	0.869	1.067	0.359	0.861
	0.4	200	0.329	0.066	0.332	0.211	0.948	1.110	0.263	0.866
	0.4	400	0.334	0.061	0.335	0.180	0.968	1.116	0.175	0.865
	0.4	1000	0.326	0.044	0.327	0.140	1.011	1.103	0.109	0.863
0.5	0.5	100	0.329	0.060	0.336	0.271	0.857	1.194	0.355	0.879
	0.5	200	0.331	0.044	0.333	0.227	0.955	1.255	0.255	0.884
	0.5	400	0.327	0.034	0.328	0.188	0.991	1.210	0.183	0.878
	0.5	1000	0.330	0.023	0.330	0.144	1.017	1.165	0.103	0.878

Table 4: Over-Identified Case, $s = 0$

h_1	h_2	T	Median Deviation		Abs. Med. Dev.		Decile Range		95% Coverage	
			$\hat{\beta}_t$	$\tilde{\beta}_{1,t}$	$\hat{\beta}_t$	$\tilde{\beta}_{1,t}$	$\hat{\beta}_t$	$\tilde{\beta}_{1,t}$	$\hat{\beta}_t$	$\tilde{\beta}_{1,t}$
0.4	0.4	100	0.003	0.003	0.149	0.219	1.001	1.204	0.801	0.889
	0.4	200	-0.002	-0.002	0.126	0.189	1.025	1.209	0.829	0.909
	0.4	400	-0.002	-0.004	0.105	0.167	1.023	1.178	0.853	0.919
	0.4	1000	0.001	-0.000	0.083	0.135	1.028	1.164	0.872	0.925
0.4	0.5	100	-0.005	-0.005	0.151	0.236	0.993	1.332	0.805	0.896
	0.5	200	-0.001	-0.001	0.125	0.202	1.013	1.270	0.829	0.908
	0.5	400	-0.002	-0.005	0.104	0.179	1.039	1.293	0.857	0.921
	0.5	1000	-0.001	-0.002	0.084	0.145	1.011	1.200	0.869	0.920
0.5	0.4	100	0.000	0.002	0.148	0.201	0.839	0.951	0.754	0.869
	0.4	200	0.002	0.004	0.122	0.169	0.903	1.009	0.761	0.868
	0.4	400	0.001	0.000	0.101	0.143	0.954	1.035	0.765	0.867
	0.4	1000	-0.000	-0.001	0.079	0.112	0.974	1.038	0.775	0.874
0.5	0.5	100	0.004	0.002	0.150	0.216	0.852	1.011	0.749	0.868
	0.5	200	-0.001	0.000	0.122	0.179	0.935	1.072	0.759	0.874
	0.5	400	0.003	0.000	0.102	0.150	0.958	1.073	0.765	0.877
	0.5	1000	-0.001	-0.001	0.079	0.117	0.970	1.044	0.772	0.879

Table 5: Over-Identified Case, $s = 0.2$

h_1	h_2	T	Median Deviation		Abs. Med. Dev.		Decile Range		95% Coverage	
			$\hat{\beta}_t$	$\tilde{\beta}_{1,t}$	$\hat{\beta}_t$	$\tilde{\beta}_{1,t}$	$\hat{\beta}_t$	$\tilde{\beta}_{1,t}$	$\hat{\beta}_t$	$\tilde{\beta}_{1,t}$
0.4	0.4	100	0.030	0.012	0.148	0.194	1.015	1.156	0.782	0.876
	0.4	200	0.034	0.011	0.121	0.167	1.009	1.145	0.812	0.891
	0.4	400	0.030	0.004	0.101	0.143	1.016	1.130	0.829	0.898
	0.4	1000	0.032	0.005	0.082	0.117	1.003	1.096	0.848	0.910
0.4	0.5	100	0.029	0.005	0.144	0.212	0.978	1.236	0.791	0.879
	0.5	200	0.030	0.007	0.122	0.179	0.997	1.226	0.811	0.891
	0.5	400	0.032	0.004	0.101	0.153	0.996	1.190	0.831	0.900
	0.5	1000	0.033	0.004	0.082	0.124	1.029	1.180	0.849	0.908
0.5	0.4	100	0.033	0.013	0.148	0.187	0.835	0.921	0.723	0.833
	0.4	200	0.029	0.001	0.120	0.154	0.914	0.985	0.739	0.846
	0.4	400	0.032	0.008	0.102	0.128	0.949	0.990	0.729	0.836
	0.4	1000	0.032	0.004	0.081	0.104	0.970	1.013	0.728	0.839
0.5	0.5	100	0.030	0.001	0.147	0.194	0.866	0.982	0.724	0.843
	0.5	200	0.035	0.012	0.123	0.162	0.915	1.018	0.730	0.847
	0.5	400	0.032	0.006	0.102	0.136	0.958	1.035	0.731	0.844
	0.5	1000	0.032	0.005	0.080	0.105	0.972	1.029	0.727	0.841

Table 6: Over-Identified Case, $s = 0.5$

h_1	h_2	T	Median Deviation		Abs. Med. Dev.		Decile Range		95% Coverage	
			$\hat{\beta}_t$	$\tilde{\beta}_{1,t}$	$\hat{\beta}_t$	$\tilde{\beta}_{1,t}$	$\hat{\beta}_t$	$\tilde{\beta}_{1,t}$	$\hat{\beta}_t$	$\tilde{\beta}_{1,t}$
0.4	0.4	100	0.231	0.061	0.244	0.188	0.996	1.101	0.513	0.834
	0.4	200	0.240	0.049	0.247	0.160	1.043	1.139	0.440	0.852
	0.4	400	0.237	0.039	0.239	0.136	1.045	1.105	0.381	0.868
	0.4	1000	0.237	0.029	0.238	0.109	1.052	1.107	0.282	0.883
0.4	0.5	100	0.237	0.045	0.250	0.198	0.984	1.156	0.506	0.845
	0.5	200	0.236	0.030	0.242	0.166	1.026	1.184	0.445	0.856
	0.5	400	0.241	0.020	0.243	0.138	1.030	1.153	0.373	0.877
	0.5	1000	0.240	0.014	0.241	0.112	1.035	1.125	0.278	0.888
0.5	0.4	100	0.232	0.063	0.249	0.184	0.904	0.940	0.443	0.793
	0.4	200	0.233	0.048	0.241	0.150	0.919	0.950	0.361	0.790
	0.4	400	0.241	0.044	0.244	0.126	0.979	0.998	0.275	0.794
	0.4	1000	0.239	0.031	0.241	0.100	0.986	0.995	0.186	0.792
0.5	0.5	100	0.230	0.047	0.246	0.185	0.863	0.917	0.446	0.803
	0.5	200	0.231	0.030	0.238	0.152	0.916	0.959	0.368	0.801
	0.5	400	0.237	0.022	0.241	0.128	0.969	0.997	0.282	0.805
	0.5	1000	0.240	0.017	0.241	0.099	0.998	0.999	0.183	0.807

Table 7: Table 7, Hausman test rejection rate at $t = T/2$

s	h_1	h_2	$T = 100$	$T = 200$	$T = 400$	$T = 1000$
0	0.4	0.4	0.013	0.024	0.015	0.019
	0.4	0.5	0.017	0.011	0.027	0.028
	0.5	0.4	0.020	0.023	0.033	0.027
	0.5	0.5	0.015	0.017	0.028	0.022
0.2	0.4	0.4	0.022	0.020	0.022	0.024
	0.4	0.5	0.021	0.023	0.031	0.029
	0.5	0.4	0.033	0.034	0.042	0.048
	0.5	0.5	0.026	0.027	0.041	0.056
0.5	0.4	0.4	0.174	0.253	0.377	0.468
	0.4	0.5	0.190	0.250	0.359	0.479
	0.5	0.4	0.282	0.422	0.529	0.652
	0.5	0.5	0.303	0.406	0.512	0.665

Table 8: Global Hausman test rejection rate, $T_0 = 5$ and $T_1 = T - 5$

s	h_1	h_2	$T = 100$	$T = 200$	$T = 400$	$T = 1000$
0	0.4	0.4	0.070	0.070	0.093	0.085
	0.4	0.5	0.062	0.071	0.074	0.100
	0.5	0.4	0.075	0.087	0.107	0.121
	0.5	0.5	0.053	0.081	0.110	0.102
0.2	0.4	0.4	0.091	0.105	0.121	0.245
	0.4	0.5	0.073	0.093	0.129	0.212
	0.5	0.4	0.090	0.121	0.159	0.258
	0.5	0.5	0.078	0.120	0.164	0.230
0.5	0.4	0.4	0.687	0.850	0.949	0.997
	0.4	0.5	0.626	0.792	0.936	0.996
	0.5	0.4	0.677	0.873	0.963	0.998
	0.5	0.5	0.668	0.835	0.952	0.997

B Narrow replication: further results

Figure 8: PC Replication, $h_1 = h_2 = 0.5$

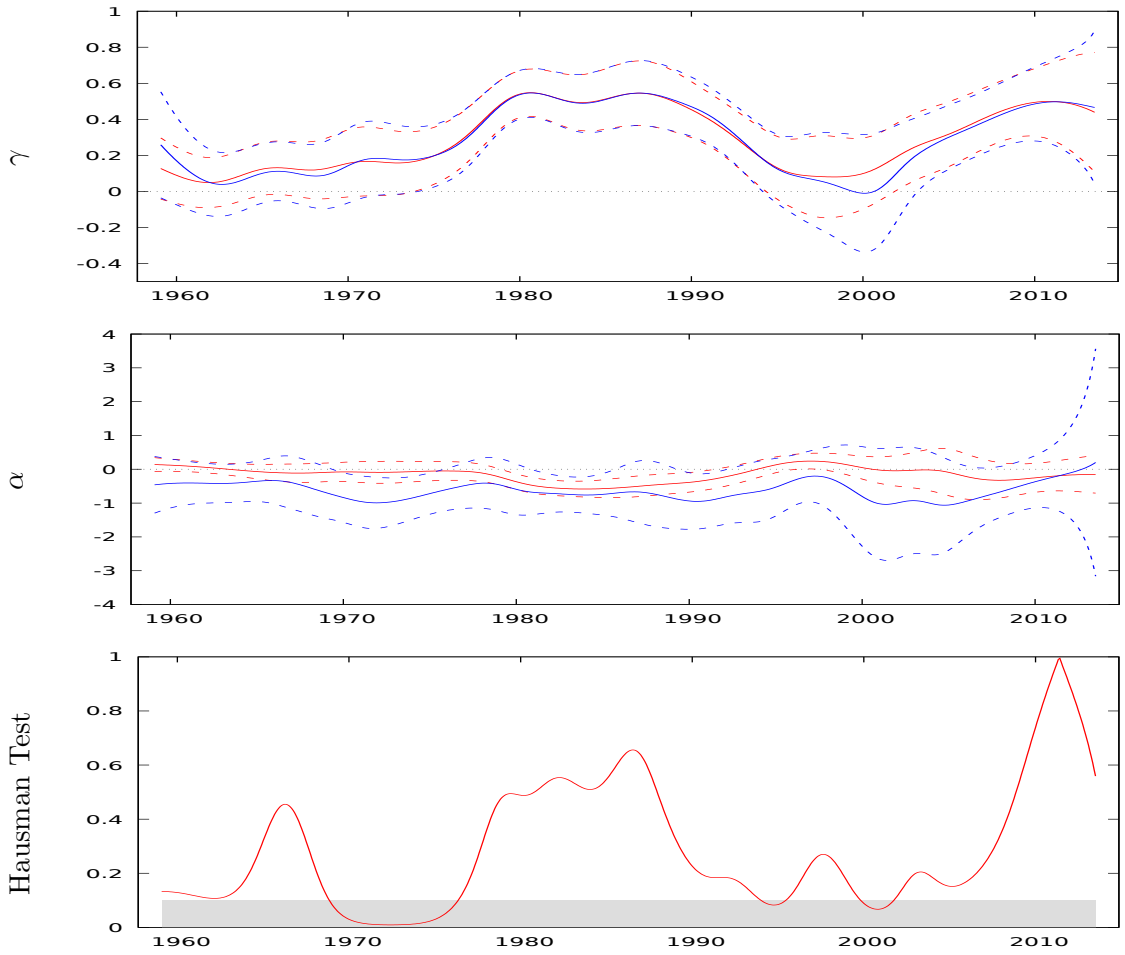

Note: see Figure 3.